World Scientific
www.worldscientific.com

# SPECTROSCOPIC STUDY OF PROPOFOL BINDING TO HUMAN SERUM ALBUMIN

SAQER M. DARWISH

*Al-Quds University, P.O. Box 20002*
*Jerusalem, Palestine, Via Israel*

The interaction of propofol and human serum albumin (HSA) has been investigated by UV-absorption, fluorescence spectroscopy and Fourier transform infrared (FT-IR) spectroscopy. Propofol has shown a strong ability to quench the intrinsic fluorescence of HSA through a static quenching procedure. The binding constant ($k$) is estimated at a low value of $2.55 \times 10^3 \, \text{M}^{-1}$ at 293 K. FT-IR spectroscopy with Fourier self-deconvolution technique was used to determine the protein secondary structure in the amide regions I, II and III. The observed spectral changes of HSA-propofol complex indicate a larger intensity decrease in the absorption band of $\alpha$-helix relative to that of $\beta$-sheets. This variation in intensity is related indirectly to the formation of H-bonding in the complex molecules, which accounts for the different intrinsic propensities of $\alpha$-helix and $\beta$-sheets.

*Keywords*: Propofol; binding constant; protein secondary structure; FT-IR spectroscopy.

## 1. Introduction

Propofol is chemically described as 2, 6-diisopropylphenol as shown in Fig. 1(a).[1] It is a short-acting intravenous anesthetic drug for controlled sedation, short surgical procedures, and maintenance of anesthesia when administered by infusion.[2,3] The clinical dose for healthy adults less than 55 years of age is 100 to 200 mcg/kg/min (6 to 12 mg/kg/h).[4] The use of propofol has been shown to restore cerebrovascular pressure autoregulation in patients during cardiopulmonary bypass.[5,6] This can be explained as a result of the cerebral vasoconstrictor effect of this drug, since vasoconstrictors are generally known to increase vascular smooth muscle tone and therefore to improve pressure autoregulation.[7] It is suggested that anesthetics drugs induce their effects in the central nervous system by binding directly to protein targets.[8] Most of these expectations come from electrophysiological measurements, coupled more recently with the techniques of molecular genetics. Even though these approaches are needed to understanding the effect of general anesthetics, they can give little information on the forces that are involved in anesthetic–protein interactions and provide no information on anesthetic binding sites.[9]
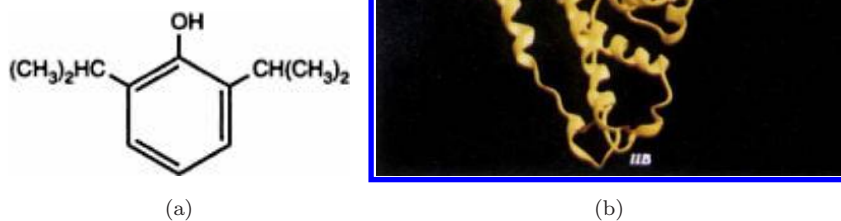
Fig. 1.    Chemical structure of propofol (a) and stereo view of HSA illustrating the overall topology and secondary structure (b).

Human serum albumin (HSA) is the most abundant protein in blood plasma which has a very effective role in transporting various compounds such as fatty acids, hormones, metabolites and large number of drugs. HSA serves as the major soluble protein constituent of the circulatory system. It contributes to colloid osmotic blood pressure, and it can bind and carry drugs which are poorly soluble in water.[10]

The three-dimensional structure of HSA is determined through X-ray crystallographic measurements shown in Fig. 1(b).[11] HSA consists of a single polypeptide chain of 585 amino acids. Its structure contains three homologous domains (labeled as I, II and III), each of which is composed of two subdomains, A and B, having six and four $\alpha$-helices, respectively.[12] The binding sites of albumin are distributed all over the molecule. Strong binding reduces the concentrations of free drugs in plasma, while weak binding can cause a short lifetime and poor distribution of the drugs. Multiple drug binding sites have been reported for HSA by several researchers.[14-19] The main binding sites for ligands in HSA are located in hydrophobic cavities in subdomains IIA and IIIA, which are labeled as site I and site II, respectively.[20] Site I is mainly known for a strong hydrophobic interaction with most neutral, bulky, heterocyclic compounds, while site II is reserved for other different interactions such as dipole–dipole, van der Waals, and/or hydrogen-bonding. HSA contained a single intrinsic tryptophan residue (Trp 214) in domain IIA and its fluorescence is sensitive to the ligands bound nearby.[21,22] Therefore, it is suitable to be used as a probe to investigate the binding properties of drugs with HSA.

According to what have been reported, more than 50% of a clinically administered general anesthetic will be bound to serum albumin, and for the binding of propofol with HSA two sites.[9] One is located in subdomain IIIA while the other is located in subdomain IIIB. In both cases the aromatic ring lies

within apolar pocket, with the phenolic hydroxyl group making a hydrogen bond with a main-chain carbonyl oxygen in case (IIIA) and with a serine hydroxyl in case (IIIB).

FT-IR spectroscopy has been a valuable method for the analysis of protein secondary structures for many years. It requires only small amounts of proteins (1 mM) in a variety of environments, to yield relatively high quality spectra. Infrared spectroscopy provides measurements of molecular vibrations due to the specific absorption of infrared radiation by chemical bonds. The form and frequency of the amide I band, which is assigned to the C=O stretching vibration within the peptide bonds is very characteristic for the structure of the studied protein.[23] From the band secondary structure, component peaks ($\alpha$-helix, $\beta$-strand) can be derived and the analysis of this single band allows elucidation of conformational changes with high sensitivity.

This work will focus on the mid-range infrared, which covers the frequency range from 4000 to 400 cm$^{-1}$. This wavelength region includes three bands that arise from the conformational sensitive vibrations within the peptide backbone namely amide I, II and III. Amide I band is the most widely used and can provide information on secondary structure composition and structural stability.

Other spectroscopy techniques are usually used in studying the interaction of drugs and proteins. Fluorescence and UV-visible spectroscopy are commonly used because of their high sensitivities, rapidity and ease of implementation. Several reports have been published studying the interaction of proteins with drugs by fluorescence techniques.[24—30]

The binding of propofol to HSA was investigated by means of UV-absorption spectroscopy, fluorescence spectroscopy, and FT-IR spectroscopy. Spectroscopic evidence regarding the drug binding mode, drug binding constant and the effects of propofol on the protein secondary structure are provided in this work.

## 2. Materials and Methods

Propofol with molecular weight 178.3 g mole$^{-1}$ in liquid form, phosphate buffer saline (pH 7.4) and HSA (fatty acid free) were purchased from Sigma chemical company and used without further purification. Phosphate buffer saline has been dissolved in distilled water before use.

### 2.1. *Preparation of stock solutions*

HSA was dissolved in phosphate buffer saline (80 mg/ml). The concentration of HSA in the buffer solution was prepared using its list molecular weight of 66.5 kDa. The solutions of propofol with the following concentrations 0.48, 0.96, 1.92, 2.88, 3.84 mM were prepared by dissolving the drug in double distilled water. In the final step drug solution was added to the protein solution of equal volume to attain the desired drug concentrations of 0.24, 0.48, 0.96, 1.44, 1.92 mM with a final protein concentration of 40 mg/ml. The propofol concentrations used in our study are in

the range and above clinical concentrations.[4] For the dry film preparation, $50\,\mu l$ of propofol and HSA solution were deposited on a silicon window and incubated for 24 hours (at 25°C) before spectroscopic measurements were taken.

## 2.2.  *UV-visible absorption spectra*

The absorption spectra were obtained by the use of a NanoDrop ND-1000 spectrophotometer. The studied samples were homogenous solutions of free HSA (40 mg/ml) and for its complexes with propofol concentrations of 0.24, 0.48, 0.96, 1.44, and 1.92 mM. The measurements were repeated for all the samples and no significant differences were observed.

## 2.3.  *Fluorescence*

The fluorescence measurements were performed by a NanoDrop ND-3300 fluorospectrometer at 25°C. The excitation source comes from one of three solid-state light emitting diodes (LEDs). The excitation source options include UV LED with maximum excitation at 365 nm, blue LED with excitation at 470 nm, and white LED from 500–650 nm excitation. A 2048-element CCD array detector covering 400–750 nm, is connected by an optical fiber to the optical measurement surface. The excitation is done at the wavelength of 360 nm and the maximum emission wavelength is at 443 nm.

## 2.4.  *FT-IR spectroscopic measurements*

All infrared spectra were recorded at room temperature on a Bruker IFS 66/S spectrophotometer equipped with a liquid nitrogen-cooled MCT detector and a KBr beam splitter. Dry film samples are prepared after two hours of incubation for the HSA and HSA-propofol solution at room temperature.

The absorption spectra were obtained in the wave number range of 4000–400 cm$^{-1}$. A spectrum was taken, using silicon windows with a spectral resolution of 4 cm$^{-1}$ and 100 scans to increase the signal-to-noise ratio. The aperture used is 8 mm, since we found that this aperture gave best signal-to-noise ratio. Baseline correction, normalization and peak areas calculations were performed for all the spectra by OPUS software. The peak positions were determined using the second derivative of the spectra.

The infrared spectra of free HSA and the propofol–HSA complexes were obtained in the region of 2500–1000 cm$^{-1}$. For the net interaction effect, the difference spectra [(protein and propofol solution) − (protein solution)] were generated using the featureless region of the protein solution 2200–1800 cm$^{-1}$ as an internal standard.[29] The accuracy of this subtraction method is tested using several control samples with the same protein or drug concentrations, which result in a flat base line formation. The obtained spectral differences were used here, to investigate the nature of the drug–HSA interaction.

## 3. Results and Discussion

### 3.1. *UV-Vis absorption spectroscopy*

The propofol–HSA binding constant is determined using UV absorption spectroscopy as reported for several drug–protein complexes.[30−32] The absorption spectra for different concentrations of propofol in HSA are shown in Fig. 2. The interaction between propofol and HSA in aqueous solution, leads to establish Eqs. (1) and (2) as follows[26]:

$$HSA + propofol \leftrightarrow propofol: HSA, \tag{1}$$
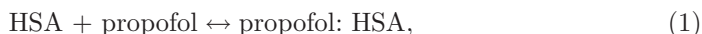
$$K = [propofol: HSA]/[propofol][HSA]. \tag{2}$$

The absorption data were treated using linear reciprocal plots based on the equation[33]

$$\frac{1}{A - A_0} = \frac{1}{A_\infty - A_0} + \frac{1}{K[A_\infty - A_0]} \cdot \frac{1}{L}, \tag{3}$$

where $A_0$ corresponds to the initial absorption of protein at 280 nm in the absence of ligand, $A_\infty$ is the final absorption of the ligated-protein, and $A$ is the recorded absorption at different propofol concentrations ($L$). The double reciprocal plot of $1/(A - A_0)$ vs $1/L$ is linear (Fig. 3) and the overall binding constant ($K$) can
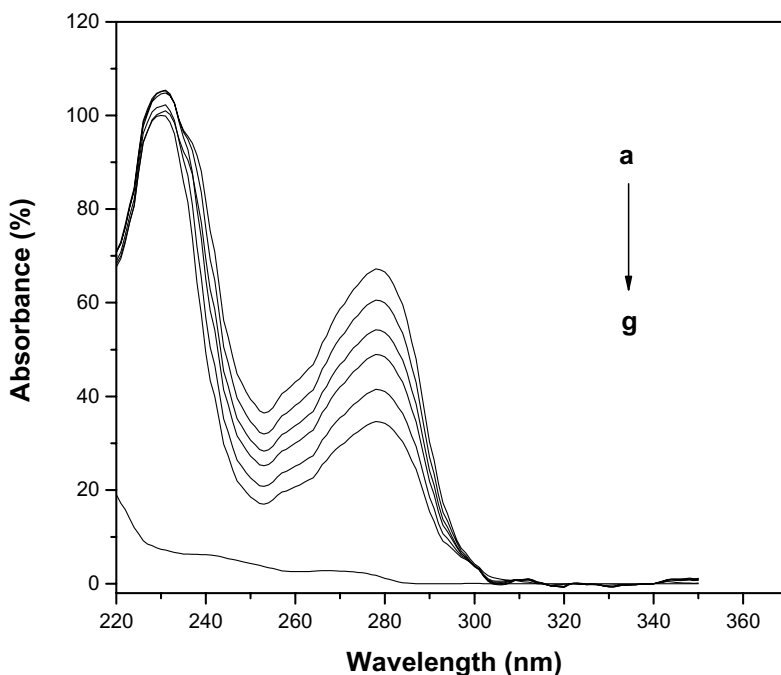


Fig. 2.   UV-absorbance spectra of HSA with different concentrations of propofol ($a = 1.92$ mM, $b = 1.44$ mM, $c = 0.96$ mM, $d = 0.48$ mM, $e = 0.24$ mM, $f = 0.00$ mM, and g propofol).
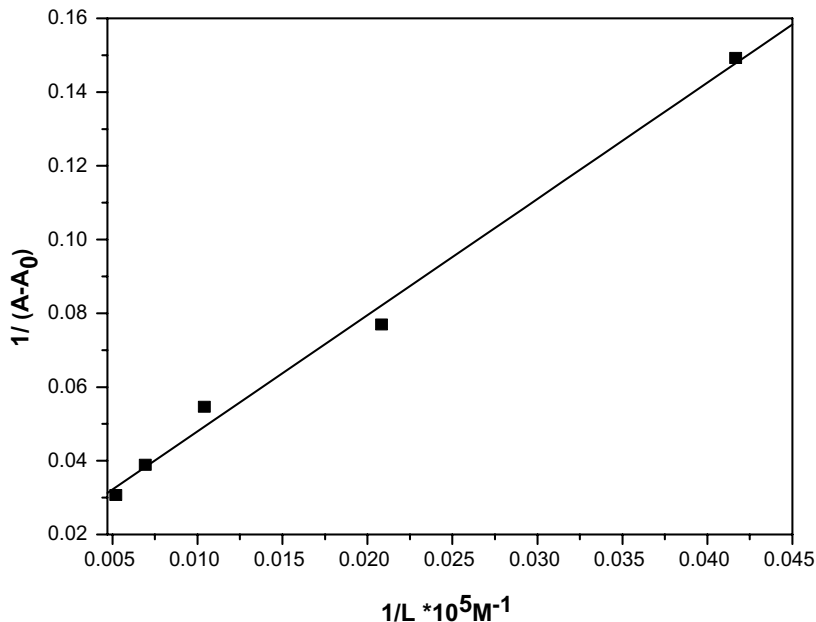
Fig. 3.   A plot of $1/(A - A_0)$ vs $1/L$ for HSA with different concentrations of propofol.

be estimated from the ratio of the intercept to the slope to be $2.55 \times 10^3 \, \text{M}^{-1}$. This binding constant value shows a relatively weak propofol–HSA interaction in comparison to other drug–HSA complexes with binding constants in the range of $10^5$ and $10^6 \, \text{M}^{-1}$.[13] It has been shown that propofol binds with highest affinity to a site in subdomain IIIA.[9] The relative weakness of the binding constant may contribute to making propofol an ultra-short-acting sedative-hypnotic agent. The reason for the low stability of the propofol–HSA complexes can be attributed to hydrogen bonding interaction between protein donor atoms and the propofol polar groups or to an indirect drug–protein interaction through water molecules.[32] It has been proposed that anesthetics may exert their effects on proteins at the molecular level by attenuating the movement of the local amino acid side chains, leading to stabilizing certain protein conformations and, hence, affecting its function.[34]

### 3.2.  *Fluorescence spectroscopy*

The fluorescence of HSA results from the tryptophan, tyrosine, and phenylalanine residues. The decrease in fluorescence of HSA is mainly attributed to change in the environment of the protein fluorophores caused by the presence of the ligand.[35] In our experiment the fluorescence sensor is based on intramolecular charge transfer (ICT), which is highly sensitive to the polarity of microenvironment.[36,37] The fluorescence emission spectra of the bound drug–HSA has been affected by the presence of ligands which bind specifically to the HSA. This leads to the use of the drug as
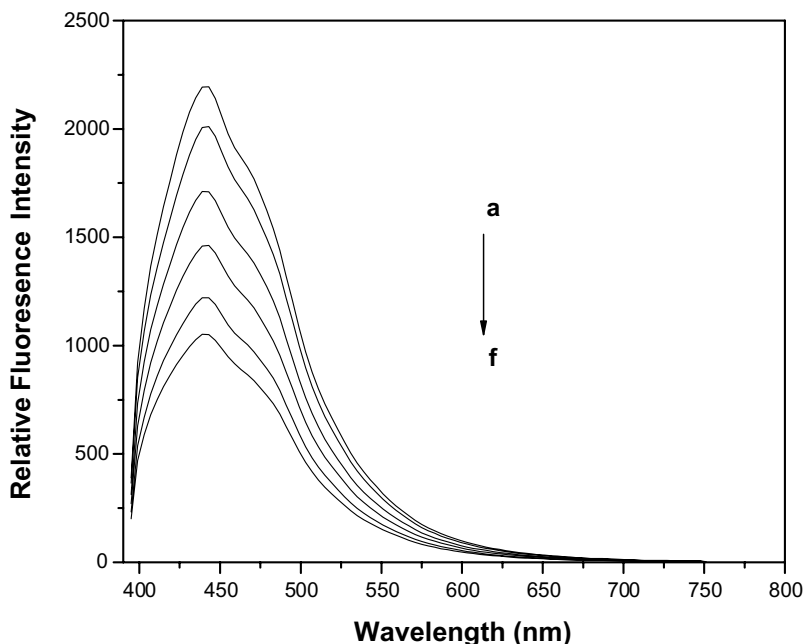
Fig. 4. Fluorescence emission spectra of HSA in the absence and presence of propofol in these concentrations ($a = 0.0\,\text{mM}$, $b = 0.24\,\text{mM}$, $c = 0.48\,\text{mM}$, $d = 0.96\,\text{mM}$, $e = 1.44\,\text{mM}$ and $f = 1.92$).

a fluorescent probe for some biochemical systems like proteins to determine the environment at the drug binding site and the binding constant between drug and HSA.[38,39] The fluorescence spectra of HSA incubated with various concentrations of propofol (0.24, 0.48, 0.96, 1.44, and 1.92 mM) are shown in Fig. 4. The fluorescence intensity of HSA decreased regularly with the increasing of propofol concentration, while the peak position shows little or no change at all indicating no change in the required bonding energy for this peak.

The dynamic quenching process can be described by the Stern–Volmer equation[24]

$$\frac{F_0}{F} = 1 + K_q \tau_0 (L) = 1 + K_{SV}(L), \tag{4}$$

where $F$ and $F_0$ are the fluorescence intensities with and without quencher, $K_q$ is the quenching rate constant of the biomolecule, $K_{SV}$ is the Stern–Volmer quenching constant, $\tau_0$ is the average lifetime of the biomolecule without quencher, and $L$ is the concentration of propofol. As can be seen from Fig. 5, the Stern–Volmer plot is linear and the slope is equal to $K_{SV}$ ($9.686 \times 10^6\,\text{L}\,\text{mol}^{-1}$). Fluorescence quenching can be induced by different mechanisms, which were usually classified into dynamic quenching and static quenching. Dynamic quenching arises from collisional encounters between the fluorophore and the quencher, and static quenching
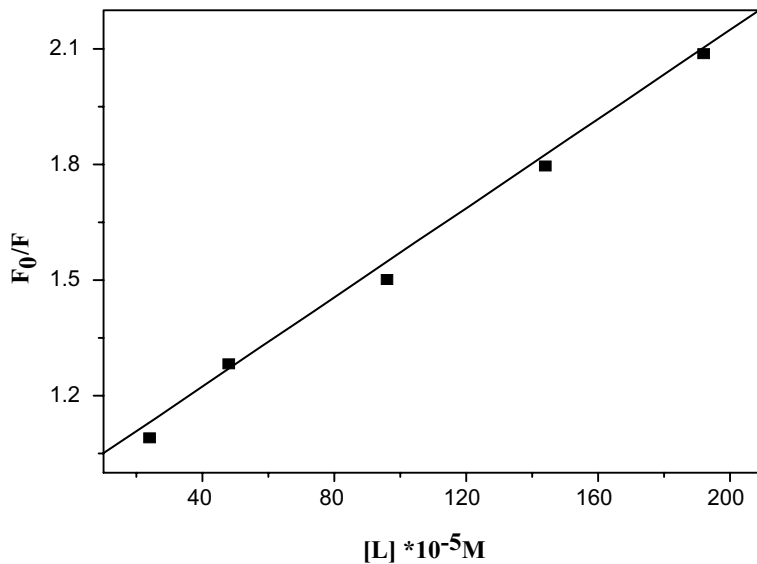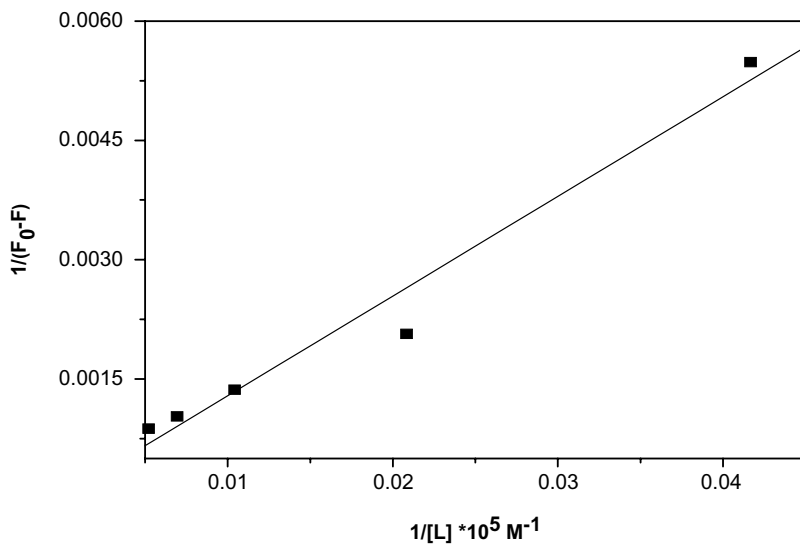
Fig. 5.    Stern–Volmer plot for propofol–HSA system.



Fig. 6.    Plot of $1/(F_0 - F)$ vs $1/[L^*10^5]$.

resulting from the formation of a ground state complex between the fluorophore and the quencher.[40]

The quenching rate constant $K_q$, can be calculated using the fluorescence lifetime of $10^{-8}$ s for HSA.[41]

The obtained value of $9.686 \times 10^{14}\,\mathrm{L\,mol^{-1}\,s^{-1}}$ is much larger than the maximum dynamic quenching constant for various quenchers with biopolymer $(2 \times 10^{10}\,\mathrm{L\,mol^{-1}\,s^{-1}})$.[42] This result confirms that a static quenching is dominant in the formed complexes.[43]

When the static quenching equation is used[40]

$$\frac{1}{F_0 - F} = \frac{1}{F_0 K(L)} + \frac{1}{F_0}, \tag{5}$$

where $K$ is the binding constant of propofol with HSA. The value of $K$ can be determined from the slope and the intercept in Fig. 6. The value of $K$ is $2.55 \times 0^3\,\mathrm{M^{-1}}$, which agrees well with the value obtained earlier by UV spectroscopy and supports the effective role of static quenching. The highly effective quenching constant in this case has lead to a lower value of binding constant between the drug and HSA suggests the formations of effective hydrogen bonding between propofol and HSA.

## 3.3. *FT-IR spectroscopy*

Infrared spectra of proteins exhibit a number of amide bands, which represent different vibrations of the peptide moiety. The amide group of proteins and polypeptides presents characteristic vibrational modes (amide modes) which are sensitive to the protein conformation and largely been constrained to group frequency interpretations.[44] Amide I ($1700–1600\,\mathrm{cm^{-1}}$) is mainly due to the C=O stretching vibration, amide II ($1600–1480\,\mathrm{cm^{-1}}$ region) is due to the coupling of the N–H in-plane bending and C–N stretching modes, and amide III ($1330–1220\,\mathrm{cm^{-1}}$ region) is attributed to the C–N stretching coupled to the in-plane N–H bending mode.[45−47] Furthermore, other bands at $1300–900\,\mathrm{cm^{-1}}$ were assigned to C–O bending modes of saccharides (glucose, lactose and glycerol), the peaks at $1430–1360\,\mathrm{cm^{-1}}$ attributed to vibrations of certain amino acids chains and $1480–1430\,\mathrm{cm^{-1}}$ is attributed to fatty acids, phospholipids and triglycerides.[48,49]

The second derivative of the FT-IR spectrum for HSA free, and the spectra for HSA with different concentrations of propofol are shown in Fig. 7, where the spectra are dominated by the absorbance bands of amide I and amide II at 1656 and $1544\,\mathrm{cm^{-1}}$, respectively. The peak positions of amide I bands in HSA infrared spectrum shifted as listed in Table 1: 1615 to $1611\,\mathrm{cm^{-1}}$, 1624 to $1627\,\mathrm{cm^{-1}}$, 1636 to $1642\,\mathrm{cm^{-1}}$, 1682 to $1678\,\mathrm{cm^{-1}}$, 1655 to $1659\,\mathrm{cm^{-1}}$ and 1695 to $1691\,\mathrm{cm^{-1}}$ after interaction with propofol. The changes of the peak positions and peak shapes demonstrated changes in the secondary structure of HSA due to its interaction with propofol. In amide II region some of the peak positions have shifted in the following order: 1543 to $1549\,\mathrm{cm^{-1}}$, 1564 to $1567\,\mathrm{cm^{-1}}$, 1577 to $1584\,\mathrm{cm^{-1}}$ and 1594 to $1597\,\mathrm{cm^{-1}}$. In the amide III region little or no change of the peak positions have been observed. The minor changes in peak positions can be attributed to the effect of the newly imposed H-bonding between the drug molecules and the protein. It is suggested that, the shift to a higher frequency for the major peak in amide I region
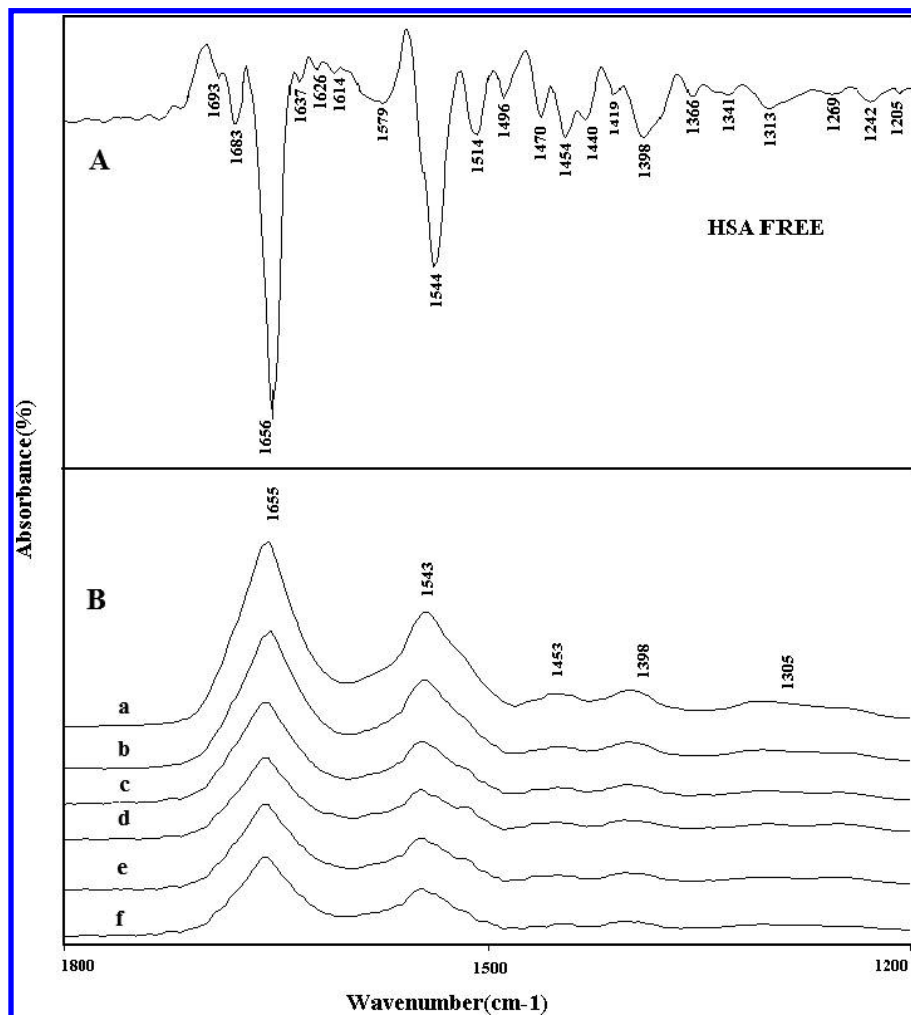
Fig. 7.   Spectra of (A) HSA-free (second derivative) and (B) shows the spectra of (a, b, c, d, e, and f) HSA–propofol with concentrations (0.0, 0.24, 0.48, 0.96, 1.44 and 1.92 mM).

(1655 to 1659) has resulted from new H-bonding, which formed as the C–N bond assumed partial double bond character due to a flow of electrons from the C=O to the C–N bond.[50]

The component bands of amide I were attributed according to the well-established assignment criterion.[51,52] The bands range 1640–1610 cm$^{-1}$ are generally assigned to $\beta$-sheet, 1650–1640 cm$^{-1}$ to random coil, 1658–1650 cm$^{-1}$ to $\alpha$-helix and 1700–1660 cm$^{-1}$ to $\beta$-turn structure. As for amide II, the absorption band consists of four components and assigned in the following order: 1500–1488 cm$^{-1}$ to $\beta$-sheets, 1525–1504 cm$^{-1}$ to random coil 1560–1527 cm$^{-1}$ to $\alpha$-helix and 1585–1564 cm$^{-1}$ to turn structure.[53] The component bands of amide III have

Table 1. Bands assignments in the absorbance spectra of HSA with different propofol concentrations for amide I–III regions.

| Bands | HSA free | HSA-prop 0.24 mM | HSA-prop 0.48 mM | HSA-prop 0.96 mM | HSA-prop 1.44 mM | HSA-prop 1.92 mM |
|---|---|---|---|---|---|---|
| Amide I (1600–1700) | 1615 | 1612 | 1611 | 1616 | 1617 | 1611 |
| | 1624 | 1627 | 1628 | 1626 | 1625 | 1627 |
| | 1636 | 1640 | 1642 | 1638 | 1637 | 1642 |
| | 1655 | 1657 | 1658 | 1657 | 1656 | 1659 |
| | 1682 | 1680 | 1677 | 1681 | 1682 | 1678 |
| | 1695 | 1692 | 1691 | 1693 | 1693 | 1691 |
| Amide II (1480–1600) | 1515 | 1515 | 1514 | 1516 | 1516 | 1514 |
| | 1532 | 1532 | 1531 | 1532 | 1532 | 1531 |
| | 1543 | 1549 | 1549 | 1548 | 1546 | 1549 |
| | 1564 | 1568 | 1566 | 1570 | 1571 | 1567 |
| | 1577 | 1583 | 1583 | 1590 | 1578 | 1584 |
| | 1594 | 1597 | 1598 | 1594 | 1592 | 1597 |
| Amide III (1220–1330) | 1226 | 1226 | 1226 | 1226 | 1226 | 1226 |
| | 1243 | 1242 | 1243 | 1243 | 1243 | 1242 |
| | 1268 | 1267 | 1269 | 1268 | 1268 | 1268 |
| | – | 1278 | 1278 | 1275 | 1275 | 1275 |
| | 1293 | 1294 | 1293 | 1294 | 1293 | 1293 |
| | 1314 | 1311 | 1313 | 1314 | 1313 | 1313 |

been assigned as follows: $\alpha$-helix 1330–1290 cm$^{-1}$, $\beta$-turn 1290–1270 cm$^{-1}$, random coil 1270–1250 cm$^{-1}$ and $\beta$-sheet 1250–1220 cm$^{-1}$.[52]

Most investigations have concentrated on amide I band assuming higher sensitivity to the change of protein secondary structure.[54] However, it has been reported that amide II band spectrum reveals enough information and could be used alone for secondary structure prediction in place of amide I.[55,56]

Others have reported that amide III is not directly affected by the strong water band and therefore it is more suited for structure determinations.[57]

The difference spectra [(protein and propofol) − (protein)] were obtained for amide I, amide II, and amide III regions to investigate the intensity variations and the results are shown in Figs. 8 and 9, respectively. In the amide I and amide II regions, two strong negative features at 1652 and 1548 cm$^{-1}$ were observed at low propofol concentration (0.48 mM). These two negative features became even stronger at higher concentrations with a little shift in their positions. In the amide III region, two strong negative features at 1242 and 1315 cm$^{-1}$ were observed at low propofol concentration and with concentration increasing these features show more strength. The observed negative features are attributed to the decrease of intensities at amide I band at 1655 cm$^{-1}$ and amide II band at 1543 cm$^{-1}$ as a result of drug interaction (H-bonding) with protein C=O and C–N groups.[26]

In this work a quantitative analysis of the protein secondary structure for the free HSA and propofol–HSA complex in dehydrated films is determined from the shape of amide I, II and III bands. Infrared Fourier self-deconvolution with second derivative resolution and curve fitted procedures,[58,59] were applied to increase
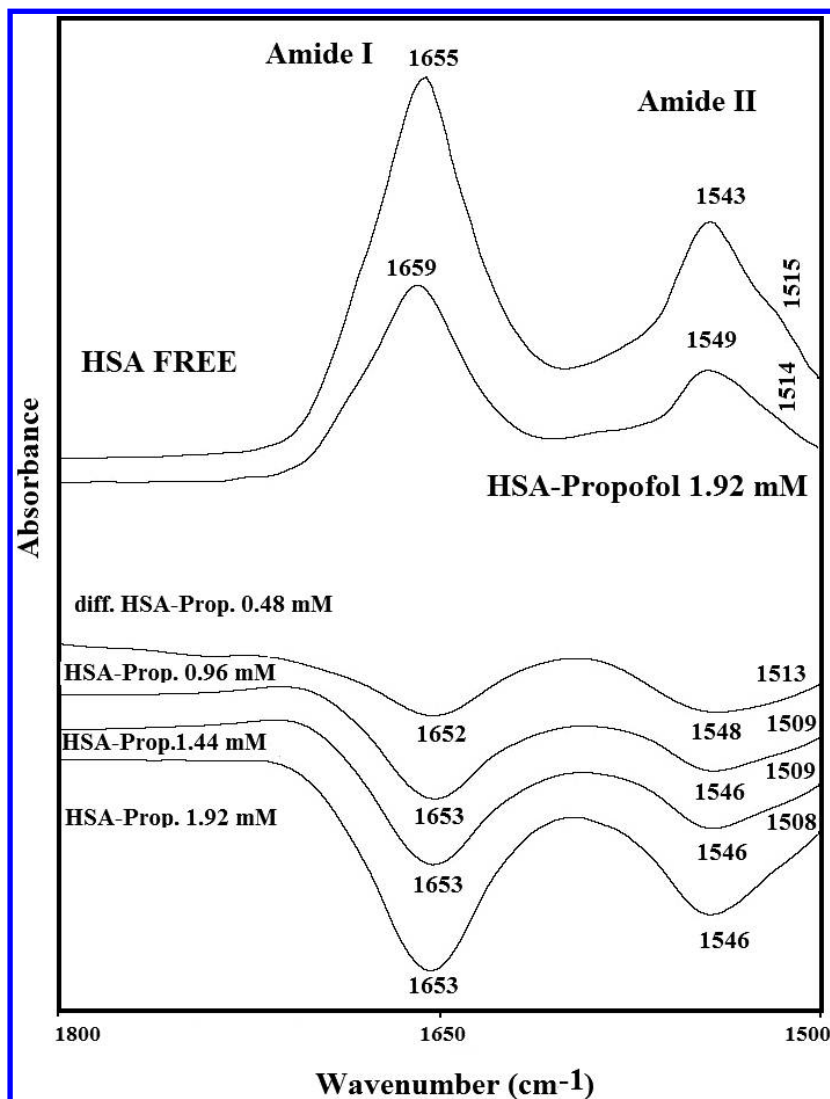
Fig. 8.   FT-IR spectra (top two curves) and difference spectra of HSA and its complexes of different propofol concentrations in the region of 1800–1500 cm$^{-1}$.

spectral resolution. Therefore it is highly effective in identifying the peak position and in determining the area of each individual band. The procedure was in general carried out considering only components detected by second derivatives and has minimum half widths at half height (HWHH) of 5 cm$^{-1}$. Based on the above band assignments, the percentages of each secondary structure of HSA were calculated from the integrated areas of the component bands in amide I, II and III respectively. Table 2 shows the content of each secondary structure of HSA before and after the interaction with propofol at different concentrations.
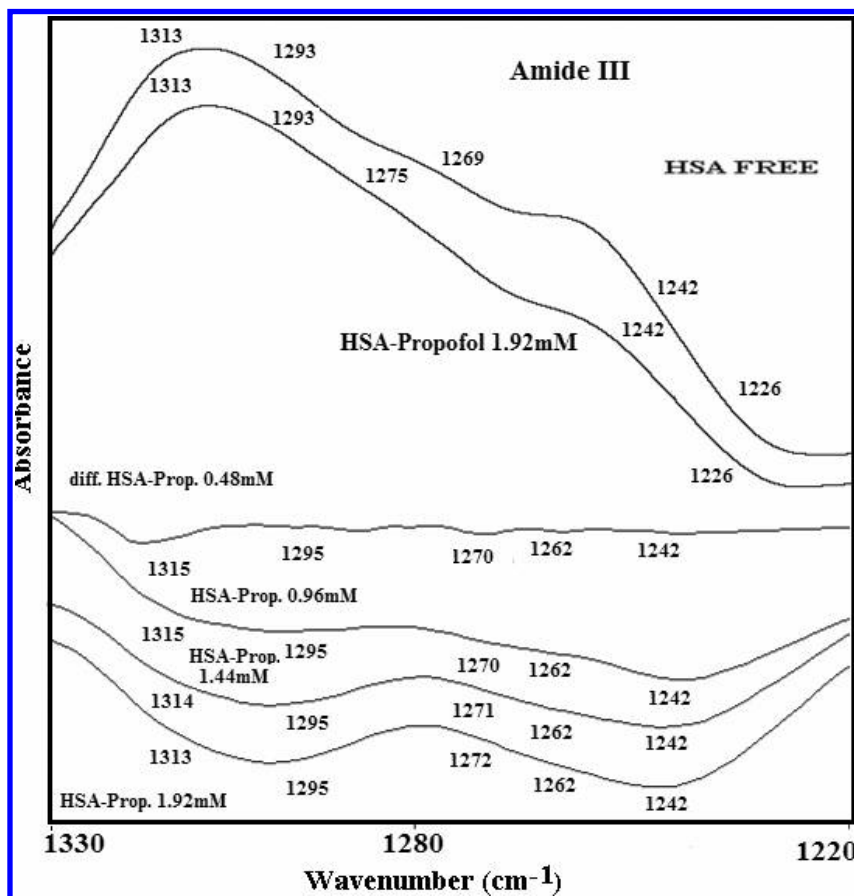
Fig. 9.    FT-IR spectra (top two curves) and the difference spectra of HSA and its complexes of different propofol concentrations in the amide III region.

Figures 10 and 11 reveal second derivative resolution enhancement and curve-fitted for amide I and amide II regions, respectively. The second derivative spectra and the secondary structure of the free human serum albumin are shown in (A, B), while its propofol complexes are shown in (C, D) for dehydrated films. It is generally accepted that infrared spectra of proteins in films and in solution may display distinct differences, but these differences are due to the presence or absence of the water or buffer molecules that imprint their mark on the spectra. It has been shown that the structural information content is of the same quality in films and in solution with an (error of <1%) for both systems.[60]

The percentage values for the components of amid I of free HSA are consistent with the results of other recent spectroscopic studies.[61–63] The results of amide II and amide III showed similar trends in their percentage values to that of amide I. The decrease of $\alpha$-helix percentage with the increase of propofol concentrations is evident in the calculations and this trend is consistent in the three

Table 2.   Secondary structure determination for amide regions (I–III) in HSA and its propofol complexes.

| Bands | HSA free | HSA-prop 0.24 mM | HSA-prop 0.48 mM | HSA-prop 0.96 mM | HSA-prop 1.44 mM | HSA-prop 1.92 mM |
|---|---|---|---|---|---|---|
| Amide I | | | | | | |
| $\beta$-sheets (cm$^{-1}$) (1603–1635) (1687–1700) | 16 | 32 | 32 | 32 | 36 | 39 |
| Random (cm$^{-1}$) (1635–1645) | 15 | 6 | 6 | 5 | 5 | 5 |
| $\alpha$-helix (cm$^{-1}$) (1648–1670) | 55 | 52 | 52 | 50 | 49 | 46 |
| Turn (cm$^{-1}$) (1670–1685) | 14 | 10 | 10 | 13 | 10 | 10 |
| Amide II | | | | | | |
| $\beta$-sheets (cm$^{-1}$) (1488–1504) (1585–1600) | 18 | 23 | 25 | 27 | 29 | 29 |
| Random (cm$^{-1}$) (1504–1525) | 14 | 15 | 14 | 14 | 15 | 15 |
| $\alpha$-helix (cm$^{-1}$) (1527–1560) | 50 | 47 | 46 | 45 | 43 | 42 |
| Turn (cm$^{-1}$) (1564–1585) | 18 | 15 | 15 | 14 | 13 | 14 |
| Amide III | | | | | | |
| $\beta$-sheets (cm$^{-1}$) (1220–1250) | 17 | 22 | 22 | 21 | 20 | 21 |
| Random (cm$^{-1}$) (1250–1270) | 15 | 15 | 16 | 16 | 17 | 17 |
| Turn (cm$^{-1}$) (1270–1290) | 18 | 18 | 18 | 20 | 21 | 21 |
| $\alpha$-helix (cm$^{-1}$) (1290–1330) | 50 | 45 | 44 | 43 | 42 | 41 |

amide regions. However, for the $\beta$-sheet the relative percentage has increased with increasing propofol concentrations. The reduction of $\alpha$-helix intensity percentage and the increase of $\beta$-sheets are speculated to be due to the unfolding of the protein in the presence of propofol as a result of the formation of H-bonding between HSA and the drug. The steric blocking effect can contribute an enthalpic stabilization to intraprotein hydrogen bonds and disfavors peptide to catalyst complexation in hydrogen exchange reactions and peptide to peptide H-bonding in the helical main chain conformation but not in $\beta$-strands.[64] The newly formed H-bonding result in the C–N bond assuming partial double bond character due to a flow of electrons from the C=O to the C–N bond which decreases the intensity of the original vibrations.[50] It seems that the H-bonding affects more of the original bonding in $\alpha$-helix than in $\beta$-sheets depending on the accessibility of the solvent and on propensities of $\alpha$-helix and $\beta$-sheets of the protein.[65] The hydrogen bonds in $\alpha$-helix are formed inside the helix and parallel to the
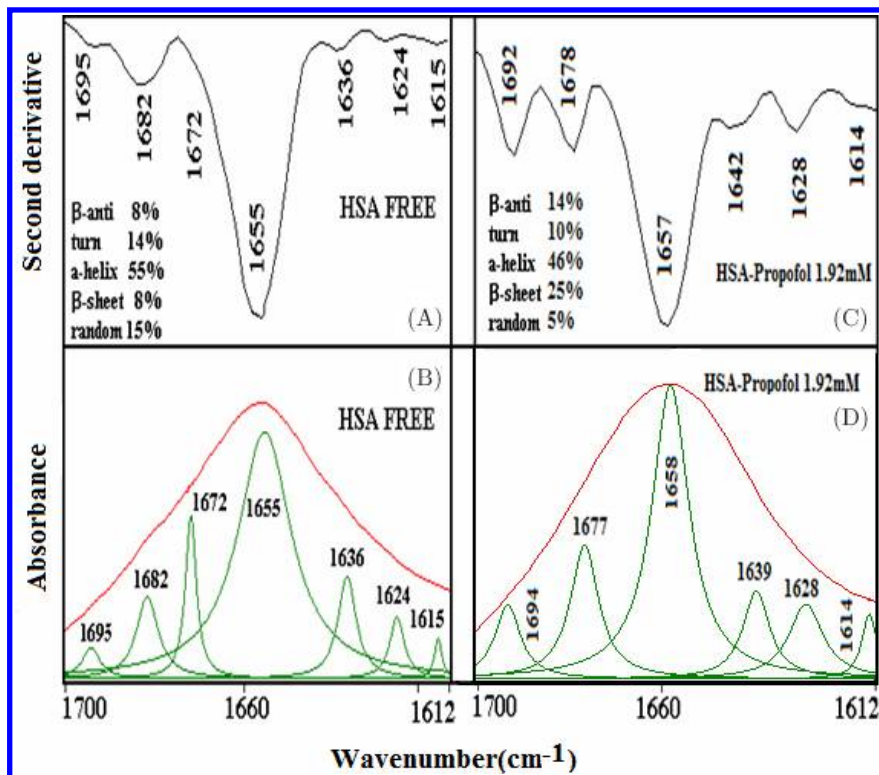
Fig. 10. Second-derivative resolution enhancement and curve-fitted amide I region (1700–1612 cm$^{-1}$) and secondary structure determination of the free human serum albumin (A, B) and its propofol complexes (C, D) with 1.92 mM drug concentration.

helix axis, while for $\beta$-sheet the hydrogen bonds take position in the planes of $\beta$-sheets as the preferred orientations especially in the anti-parallel sheets. The restrictions on the formation of hydrogen bonds in $\beta$-sheet relative to the case in $\alpha$-helix explains the larger effect on reducing the intensity percentage of $\alpha$-helix to that of $\beta$-sheet. Similar conformational transitions from an $\alpha$-helix to $\beta$-sheet structure were reported for the protein unfolding upon protonation and heat denaturation.[66,67]

In summary, the binding of propofol to HSA has been investigated by UV-visible absorption spectroscopy, fluorescence spectroscopy and by FT-IR spectroscopy. From the UV and fluorescence investigations we determined values for the binding constant and the quenching constant. The results indicate that the intrinsic fluorescence of HSA was quenched by propofol through static quenching mechanism. Analysis of the FT-IR spectra in the three amide regions (I, II and III) reveals that HSA–propofol interaction induces intensity reduction in the absorption bands of $\alpha$-helix and $\beta$-sheets components with different proportionality due to the different accessibility of H-bond formation in these components.
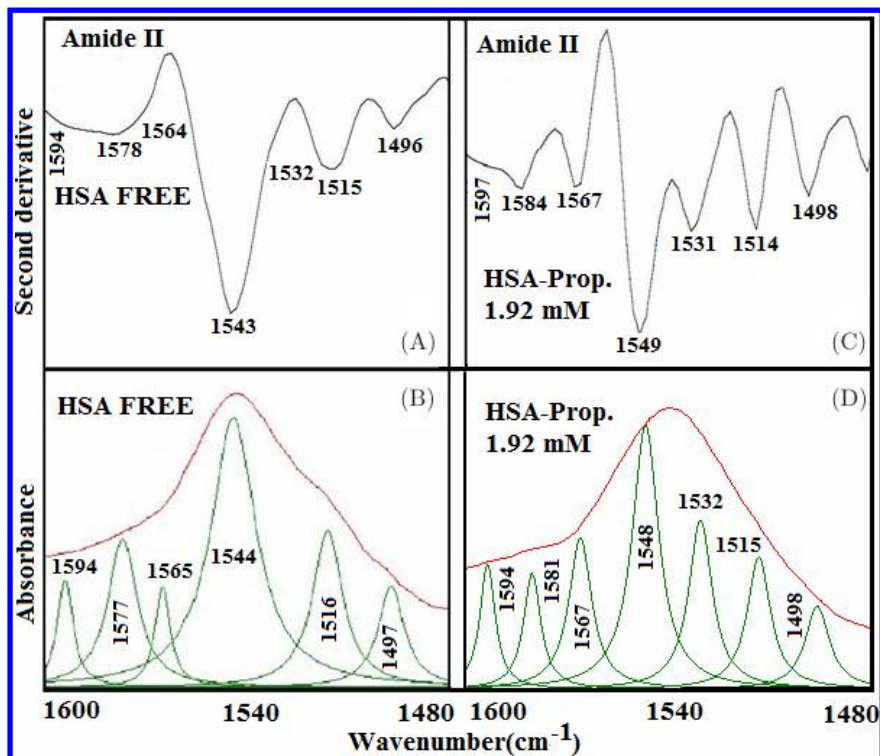
Fig. 11.   Second-derivative resolution enhancement and curve fitted amide II $(1600–1480\,cm^{-1})$ and secondary structure determination of the free human serum albumin (A, B) and its propofol complexes (C, D) with 1.92 mM drug concentration.

## Acknowledgments

## References

1. G. Edward Morgan, M. S. Mikhail and M. J. Murry, *Clinical Anesthesiology*, 4th edn. (McGraw-Hill, 2006).
2. M. Langley and R. Heel, *Drugs* **35**, 334 (1988).
3. G. Trapani, C. Altomare, G. Liso, E. Sanna and G. Biggio, *Curr. Med. Chem.* **7**, 249 (2000).
4. J. Pershad, J. Wan and D. L. Anghelescu, *Pediatrics* **120**, 629 (2007).
5. J. M. Harrison, K. J. Girling and R. P. Mahajan, *Br. J. Anaesth.* **83**, 839 (1999).
6. S. Ederberg, A. Westerlind and E. Houltz, *Anesth. Analg.* **86**, 1201 (1998).
7. J. M. Chillon and G. L. Baumbach, Autoregulation, arterial and intracranial pressure, in *Cerebral Blood Flow and Etabolism*, L. Edvinsson and D. N. Krause, eds. (Lippincott Williams & Wilkins, Philadelphia, 2002), pp. 395–412.
8. N. P. Franks and W. R. Lieb, *Nature* **367**, 607 (1994).
9. A. A. Bhattacharya, S. Curry and N. P. Franks, *J. Biol. Chem.* **275**(49), 38731 (2000).

10. T. Peters, *Adv. Protein Chem.* **37**, 161 (1985).
11. X. M. He and D. C. Carter, *Nature* **358**, 209 (1992).
12. S. Curry, P. Brick and N. P. Franks, *Biochim. Biophys. Acta.* **1441**, 131 (1999).
13. U. Kragh-Hansan, *Pharmacol. Rev.* **33**, 17 (1981).
14. K. Oettl and R. E. Stauber, *Br. J. Pharmacol.* **151**, 580 (2007).
15. U. Kragh-Hansen, V. T. G. Chuang and M. Otagiri, *Biol. Pharm. Bull.* **25**, 695 (2002).
16. G. Sudlow, D. J. Birkett and D. N. Wade, *Mol. Pharmacol.* **11**, 824 (1975).
17. F. Shin-Ichi and A. Takashi, *Biophys. J.* **94**, 95 (2008).
18. K. H. Ulrich, W. Hiroshi, N. Keisuke, I. Yasunori and O. Masaki, *J. Mol. Biol.* **363**, 702 (2006).
19. A. Bhattacharya, T. Gruene and S. Curry, *J. Mol. Biol.* **303**, 721 (2000).
20. S. Curry, H. Mandelkow, P. Brick and N. Franks, *Nat. Struct. Biol.* **5**, 827 (1998).
21. S. S. Krishnakumar and D. Panda, *Biochemistry* **41**, 7443 (2002).
22. Y. V. Il'ichev, J. L. Perry and J. D. Simon, *J. Phys. Chem. B* **106**, 460 (2002).
23. S. Krimm and J. Bandekar, *Adv. Protein Chem.* **38**, 181 (1986).
24. J. N. Tian, J. Q. Liu, J. Y. Zhang, Z. D. Hu and X. G. Chen, *Chem. Pharm. Bull.* **51**, 579 (2003).
25. J. Sereikaite and V. A. Bumelis, *Acta Biochim. Pol.* **53**, 87 (2006).
26. M. Purcell, J. F. Neault and H. A. Tajmir-Riahi, *Biochim. Biophys. Acta* **1478**, 61 (2000).
27. T. Jianghong, L. Ning, H. Xianghong and Z. Guohua, *J. Mol. Struct.* **889**, 408 (2008).
28. J. Li, C. Ren, Y. Zhang, X. Liu, X. Yao and Z. Hu, *J. Mol. Struct.* **881**, 90 (2008).
29. W. K. Surewicz, H. H. Mantsch and D. Chapman, *Biochemistry* **32**, 389 (1993).
30. J. J. Stephanos, *J. Inorg. Biochem.* **62**, 155 (1996).
31. M. I. Klotz and L. D. Hunston, *Biochemistry* **10**, 3065 (1971).
32. I. M. Klotz, *Science* **217**, 1247 (1982).
33. J. S. Johansson, H. Zou and J. W. Tanner, *Anesthesiology* **90**, 235 (1999).
34. J. Stephanos, S. Farina and A. Addison, *Biochemica. Biophysica. Acta* **1295**, 209 (1996).
35. A. Sulkowaska, *J. Mol. Strurct.* **614**, 227 (2002).
36. F.-Y. Wu, Z.-J. Ji, Y.-M. Wu and X.-F. Wan, *Chem. Phys. Lett.* **424**, 387 (2006).
37. J. K. Amisha Kamal, L. Zhao and A. H. Zewail, *Proc. Natl. Acad. Sci.: USA* **101**, 13411 (2004).
38. T. Gao, Y. X. Ci, H. Y. Jian and C. An, *Vibrat. Spectros.* **24**, 225 (2000).
39. V. A. Sirotkin, A. N. Zinatullin, B. N. Solomonov, D. A. Faizullin and V. D. Fedotov, *Biochim. Biophys. Acta* **1547**, 359 (2001).
40. J. R. Lakowicz, *Principles of Fluorescence Spectroscopy*, 2nd edn. (Kluwer Academic Publishers/Plenum Press, New York, 1999).
41. G. Z. Chen, X. Z. Huang, J. G. Xu, Z. Z. Zheng and Z. B. Wang, *Method of Fluorescence Analysis*, 2nd edn. (Science Press, Beijing, 1990).
42. J. R. Lakowicz and G. Weber, *Biochemistry* **12**, 4161 (1973).
43. T. Wang, B. Xiang, Y. Wang, C. Chen, Y. Dong, H. Fang and M. Wang, *Colloids Surf. B* **65**, 113 (2008).
44. Z. Ganim and A. Tokmakoff, *Biophys. J.* **91**, 2636 (2006).
45. V. A. Sirotkin, A. N. Zinatullin, B. N. Solomonov, D. A. Faizullin and V. D. Fedotov, *Biochim. Biophys. Acta* **1547**, 359 (2001).
46. R. K. Dukor, Vibrational spectroscopy in the detection of cancer, in *Handbook of Vibrational Spectroscopy*, J. M. Chalmers and P. R. Griffiths (eds.) (John Wiley and Sons, Chickchester, 2001), pp. 3335–3360.
47. Y. N. Chirgadze, O. V. Fedorov and N. P. Trushina, *Biopolymers* **14**, 679 (1975).

48. G. Deleris and C. Petibios, *Vibrat Spectrosc.* **32**, 129 (2003).
49. E. Bramanti and E. Benedetti, *Biopolymers* **38**, 639 (1996).
50. M. Jackson and H. H. Mantsch, *Can. J. Chem.* **69**, 1639 (1991).
51. D. M. Byler, J. N. Brouilette and H. Susi, *Spectroscopy* **1**, 39 (1986).
52. M. Jiang, M. X. Xie, D. Zheng, Y. Liu, X. Y. Li and X. Chen, *J. Mol. Struct.* **692**, 71 (2004).
53. A. I. Ivanov, R. G. Zhbankov, E. A. Korolenko, E. V. Korolik, L. A. Meleshchenko, M. Marchewka and H. Ratajczak, *J. Appl. Spectrosc.* **60**, 305 (1994).
54. K. Rahmelow and W. Hubner, *Anal. Biochem.* **241**, 5 (1996).
55. E. Goormaghtigh, R. Jean-Marie and V. Raussens, *Biophys. J.* **90**, 2946 (2006).
56. K. A. Oberg, J. M. Ruysschaert and E. Goormaghtigh, *Eur. J. Biochem.* **271**, 2937 (2004).
57. F. N. Fu, D. B. DeOliveira, W. R. Trumble, H. K. Sarkar and B. R. Singh, *Appl. Spectrosc.* **48**, 1432 (1994).
58. M. Byler and H. Susi, *Biopolymers* **25**, 469 (1986).
59. E. Goormaghtigh, V. Cabiaux and J. M. Ruysschaert, *Eur. J. Biochem.* **193**, 409 (1990).
60. E. Goormaghtigh, V. Raussens and J. M. Ruysschaert, *Biochim. Biophys. Acta.* **1422**, 105 (1999).
61. A. Ahmed Ouameur, E. Mangier, S. Diamantoglou, R. Rouillon, R. Carpentier and H. A. Tajmir-Riahi, *Biopolymers* **73**, 503 (2004).
62. R. Beauchemin, C. N. N'soukpoe-Kossi, T. J. Thomas, T. Thomas, R. Carpentier and H. A. Tajmir-Riahi, *Biomacromolecules* **8**, 3177 (2007).
63. S. M. Darwish *et al.*, *J. Mol. Struct.* (2009), doi: 10.1016/j. Molstruc, 2009.10.023
64. Y. Bai and S. W. Englander, *Proteins* **18**, 262 (1994).
65. C. A. Kim and J. M. Berg, *Nature* **362**, 267 (1993).
66. F. S. Parker, *Applications of Infrared, Raman and Resonance Spectroscopy in Biochemistry* (Plenum, New York, 1983).
67. I. E. Holzbaur, A. M. English and A. A. Ismail, *Biochemistry* **35**, 5488 (1996).